

The 4th Symposium on Computational Marine Hydrodynamics, 2021
第四届CMHL 船舶与海洋工程计算水动力学研讨会

Nonlinear Seakeeping Solution near the Critical Frequency

Yuming Liu (yuming@mit.edu)

Center for Ocean Engineering
Department of Mechanical Engineering
Massachusetts Institute of Technology
January 14, 2021



Massachusetts Institute of Technology

Applications of Nonlinear Wave Hydrodynamics

Calculation of wave induced loads of ships and offshore structures is a classical problem.

- For most cases, linear theory is valid under small wave steepness assumption.
- Nonlinearity is important for bodies with large-amplitude motions or in steep waves or solutions obtained by linear theory is trivial or singular.
- For instance, a body moving with forward speed U and oscillate with angular velocity ω is often approximated as source points with linearized velocity potential (Haskind 1954):

$$\phi(x, z) \sim \frac{\epsilon}{\sqrt{1 - 4\tau}}$$

Here ϵ = wave steepness;

$\tau \equiv \frac{U\omega}{g}$: when $\tau \rightarrow \frac{1}{4}$, the solution becomes infinity, which is known as the **critical frequency**.

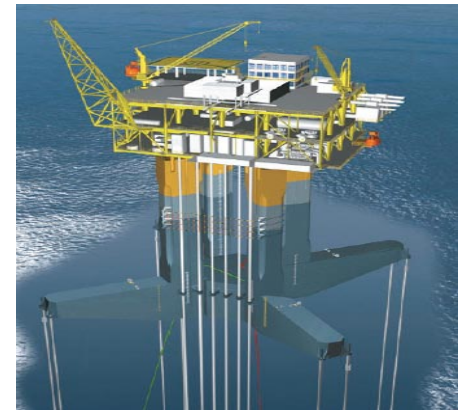
Applications of Nonlinear Wave Hydrodynamics

- Stability and global performance analysis of ship with forward speed:

➤ The combination of ship velocity U and the encounter wave frequency ω_e satisfies $\tau = \frac{U\omega_e}{g} \approx \frac{1}{4}$.

- Hydrodynamic loads on offshore structures (e.g. TLP, FPSO, LNG) due to current-wave induced motions:

➤ The average current speed in Gulf of Mexico is $U_{current} = 0.3 \sim 1.2 \text{ m/sec}$ (Data from NODC); the natural period of TLP in heave mode is $T_{heave} = 2 \sim 3 \text{ sec}$ (Johannessen, 2006), leading to $\tau \equiv \frac{U\omega}{g} = \frac{2\pi U_{current}}{gT_{heave}} \approx \frac{1}{4}$

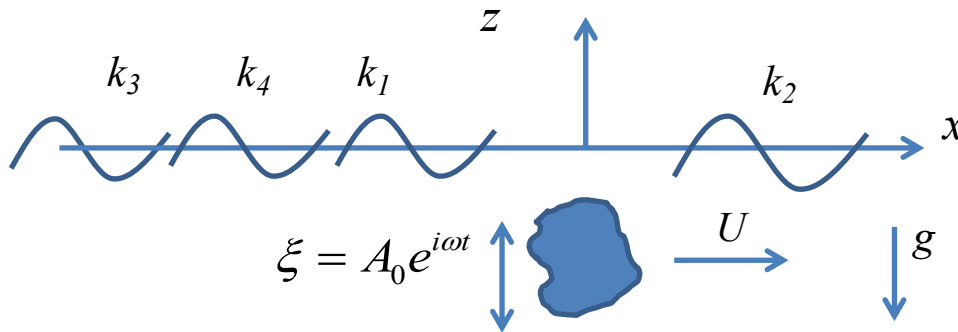


Research Purposes

- Understand the role of body geometry and nonlinearity in the seakeeping solution near the critical frequency with $\tau \equiv \frac{U\omega}{g} = \frac{1}{4}$
 - Develop theoretical analysis in the frequency domain to understand the effect of nonlinearity on the seakeeping solutions for a two- and three-dimensional bodies
 - Apply independent time-domain numerical nonlinear simulations to validate the theoretical analysis
1. LIU, Y. & YUE, D. K. P. 1993 On the solution near the critical frequency for an oscillating and translating body in or near free surface. *J. Fluid Mech.* **254**, pp 251–266.
 2. Liu, Y. & Yue, D. K. P. 1996 On the time dependence of the wave resistance of a body accelerating from rest. *J. Fluid Mech.* **310**, pp 331-363
 3. LI, C. & LIU, Y. 2018 On the weakly nonlinear seakeeping solution near the critical frequency. *J. Fluid Mech.* **846**, pp 999-1022.

Background

- Wave generation by an oscillating body with a forward speed:



- $\tau < \frac{1}{4}$,
 k_1, k_3, k_4 = downstream waves;
 k_2 = upstream wave
- $\tau > \frac{1}{4}$,
 k_3, k_4 = downstream wave
- At Critical Frequency $\tau = \frac{1}{4}$,**
 k_3, k_4 = downstream wave;
 k_1, k_2 merge into a single wave with group velocity $V_g = U$. Wave energy cannot radiate away from the body.
Linear solution at $\tau = \frac{1}{4}$ may be singular.

- Non-Dimensional Frequency:

$$\tau \equiv \frac{U\omega}{g}$$

Existing Knowledge

(A) Linear Solution for a Single Point Source (Haskind, 1954):

$$\phi(x, z) \sim \frac{\epsilon}{\sqrt{1 - 4\tau}} = \frac{\epsilon}{\delta}$$

- As $\delta = \sqrt{1 - 4\tau} \rightarrow 0$, the velocity potential becomes singular.

(B) Nonlinear Solution for a Single Point Source (Dagan & Miloh, 1982):

$$\phi(x, z) \sim \frac{\epsilon}{\sqrt{\delta^2 + \sqrt{\delta^4 + \epsilon^2}}}$$

- As $\delta = \sqrt{1 - 4\tau} \rightarrow 0$, the velocity potential remains finite, and is proportional to $O(\epsilon^{1/2})$.

(C) Linear Solution for Actual Bodies (e.g. Grue & Palm 1984)

- Frequency-domain numerical solution for a submerged circular cylinder indicates that the linear solution is $O(\epsilon)$ and finite. No theoretical proof was provided.

Q: (1) Proof of a finite linear solution for a real body?

(2) What is the effect of *nonlinearity* in the case for real bodies?

Linearized Boundary-Value Problem

$$\Phi^*(x, z, t) = \bar{\phi}(x, z) + \Phi(x, z, t) = \bar{\phi}(x, z) + \text{Re}\{\phi(x, z)e^{i\omega t}\}$$

Field equation: $\phi_{xx} + \phi_{zz} = 0$

Linearized free-surface boundary condition:

$$(i\omega - U \frac{\partial}{\partial x})^2 \phi + g \frac{\partial \phi}{\partial z} = 0 \quad \text{on } z = 0$$

Body boundary condition:

$$\frac{\partial \phi}{\partial n} = f(x, z) \quad \text{on } S_B$$

Deepwater condition:

$$\nabla \phi \rightarrow 0 \quad \text{as } z \rightarrow -\infty$$

Green Function

Haskind (1954):

$$G(x, z; x', z') = G_0 + G_1 + G_2 + G_3 + G_4,$$

where

$$G_0 = \frac{1}{2} \{ \ln[(x - x')^2 + (z - z')^2] - \ln[(x - x')^2 + (z + z')^2] \}$$

$$G_1 = \frac{i\pi}{(1 - 4\tau)^{\frac{1}{2}}} e^{k_1[-i(x-x')+(z+z')]} + \frac{1}{(1 - 4\tau)^{\frac{1}{2}}} \int_0^\infty \frac{1}{m - k_1} e^{m[-i(x-x')+(z+z')]} dm,$$

$$G_2 = \frac{i\pi}{(1 - 4\tau)^{\frac{1}{2}}} e^{k_2[-i(x-x')+(z+z')]} - \frac{1}{(1 - 4\tau)^{\frac{1}{2}}} \int_0^\infty \frac{1}{m - k_2} e^{m[-i(x-x')+(z+z')]} dm,$$

$$G_3 = \frac{-i\pi}{(1 + 4\tau)^{\frac{1}{2}}} e^{k_3[i(x-x')+(z+z')]} + \frac{1}{(1 + 4\tau)^{\frac{1}{2}}} \int_0^\infty \frac{1}{m - k_3} e^{m[i(x-x')+(z+z')]} dm,$$

$$G_4 = \frac{i\pi}{(1 + 4\tau)^{\frac{1}{2}}} e^{k_4[i(x-x')+(z+z')]} - \frac{1}{(1 + 4\tau)^{\frac{1}{2}}} \int_0^\infty \frac{1}{m - k_4} e^{m[i(x-x')+(z+z')]} dm,$$

$$k_{1,2} = \frac{\kappa}{8\tau^2} (1 - 2\tau \pm (1 - 4\tau)^{\frac{1}{2}}); \quad k_{3,4} = \frac{\kappa}{8\tau^2} (1 + 2\tau \pm (1 + 4\tau)^{\frac{1}{2}});$$

$$\tau \equiv U\omega/g$$

$$\kappa \equiv 4\omega^2/g$$

Asymptotic Expansion of Green Function near $\tau = 1/4$

For convenience, we define $\delta^2 \equiv |1 - 4\tau|$. For $\delta^2 \ll 1$, we have

$$k_{1,2} = \kappa[1 + O(\delta)], \quad \delta^2 \ll 1$$

$$G_1 + G_2 = \frac{2\pi i}{\delta} e^{\kappa[-i(x-x')+(z+z')]} + G' + O(\delta), \quad \delta^2 \ll 1.$$

$$\frac{1}{4}G' + 1 = \kappa[-i(x-x') + (z+z')] e^{\kappa[-i(x-x')+(z+z')]} \int_{-\kappa}^{\infty} \frac{1}{m} e^{m[-i(x-x')+(z+z')]} dm$$

G_3 and G_4 are regular and $O(1)$

Solution for a Submerged Body near $\tau = 1/4$

Using source formulation:

$$\phi(x, z) = \int_{S_B} \sigma(x', z') G(x, z; x', z') ds'$$

Imposing the body boundary condition to find unknown source distribution σ :

$$\pi\sigma(x, z) + \int_{S_B} \sigma(x', z') \frac{\partial}{\partial n} G(x, z; x', z') ds' = f(x, z), \quad (x, z) \in S_B$$

In the neighborhood of $\tau = \frac{1}{4}$:

$$\begin{aligned} \pi\sigma(x, z) + \frac{2\pi\kappa}{\delta} (n_x + in_z) e^{\kappa(-ix+z)} \int_{S_B} \sigma(x', z') e^{\kappa(ix'+z')} ds' \\ + \int_{S_B} \sigma(x', z') \tilde{G}_n(x, z; x', z') ds' = f(x, z) + O(\delta), \quad \delta^2 \ll 1 \end{aligned}$$

We now define the Kochin function

$$\alpha \equiv \int_{S_B} \sigma(x, z) e^{\kappa(ix+z)} ds$$

$$\begin{aligned} \text{Then, } \sigma(x, z) = -\frac{2\kappa\alpha}{\delta} (n_x + in_z) e^{\kappa(-ix+z)} \\ - \frac{1}{\pi} \int_{S_B} \sigma(x', z') \tilde{G}_n(x, z; x', z') ds' + \frac{f(x, z)}{\pi} + O(\delta), \quad \delta^2 \ll 1 \end{aligned}$$

$$\alpha = \frac{\delta}{\pi(\delta + 2i\kappa\Gamma)} [\mathcal{F} - \int_{S_B} \sigma(x', z') P(x', z') ds'] + O(\delta^2),$$

where the kernel P is given by

$$P(x', z') = \int_{S_B} e^{\kappa(ix+z)} \frac{\partial}{\partial n} (G' + G_0) ds,$$

and the constants \mathcal{F} and Γ are given by

$$\mathcal{F} = \int_{S_B} f(x, z) e^{\kappa(ix+z)} ds, \quad \Gamma = \int_{S_B} (-in_x + n_z) e^{2\kappa z} ds$$

For $\Gamma \neq 0$,

$$\begin{aligned} \pi\sigma(x, z) - \frac{(n_x + in_z)}{\delta/2\kappa + i\Gamma} e^{\kappa(-ix+z)} \int_{S_B} \sigma(x', z') P(x', z') ds' \\ + \int_{S_B} \sigma(x', z') \tilde{G}_n(x, z; x', z') ds' = F(x, z) + O(\delta), \end{aligned}$$

where

$$F(x, z) = f(x, z) - \mathcal{F} \frac{(n_x + in_z)}{\delta/2\kappa + i\Gamma} e^{\kappa(-ix+z)} = O(1).$$

$$\sigma = O(1), \quad \alpha = O(\delta)$$

$$\phi(x, z) = \frac{2\pi i\alpha}{\delta} e^{\kappa(-ix+z)} + \int_{S_B} \sigma(x', z') \tilde{G}(x, z; x', z') ds' + O(\delta) = O(1)$$

For $\Gamma = 0$, $\alpha = O(1)$, $\sigma = O(\delta^{-1})$, $\phi = \text{unbounded}$

Body Geometry Parameter

$$\Gamma \equiv \int_{S_B} (-in_x + n_z)e^{2\kappa z} ds$$

With the use of the divergence theorem, we obtain immediately

$$\Gamma = 2\kappa \iint_B e^{2\kappa z} dS ,$$

where B is the (mean) body section. Since the integrand in (3.14) is positive definite, $\Gamma \neq 0$ if and only if the (submerged) body has non-zero cross-section area. The known singular solution for a point source turns out to be a special case of $\Gamma = 0$.

Comparison of Theoretical Solution with Direct Numerical Computation

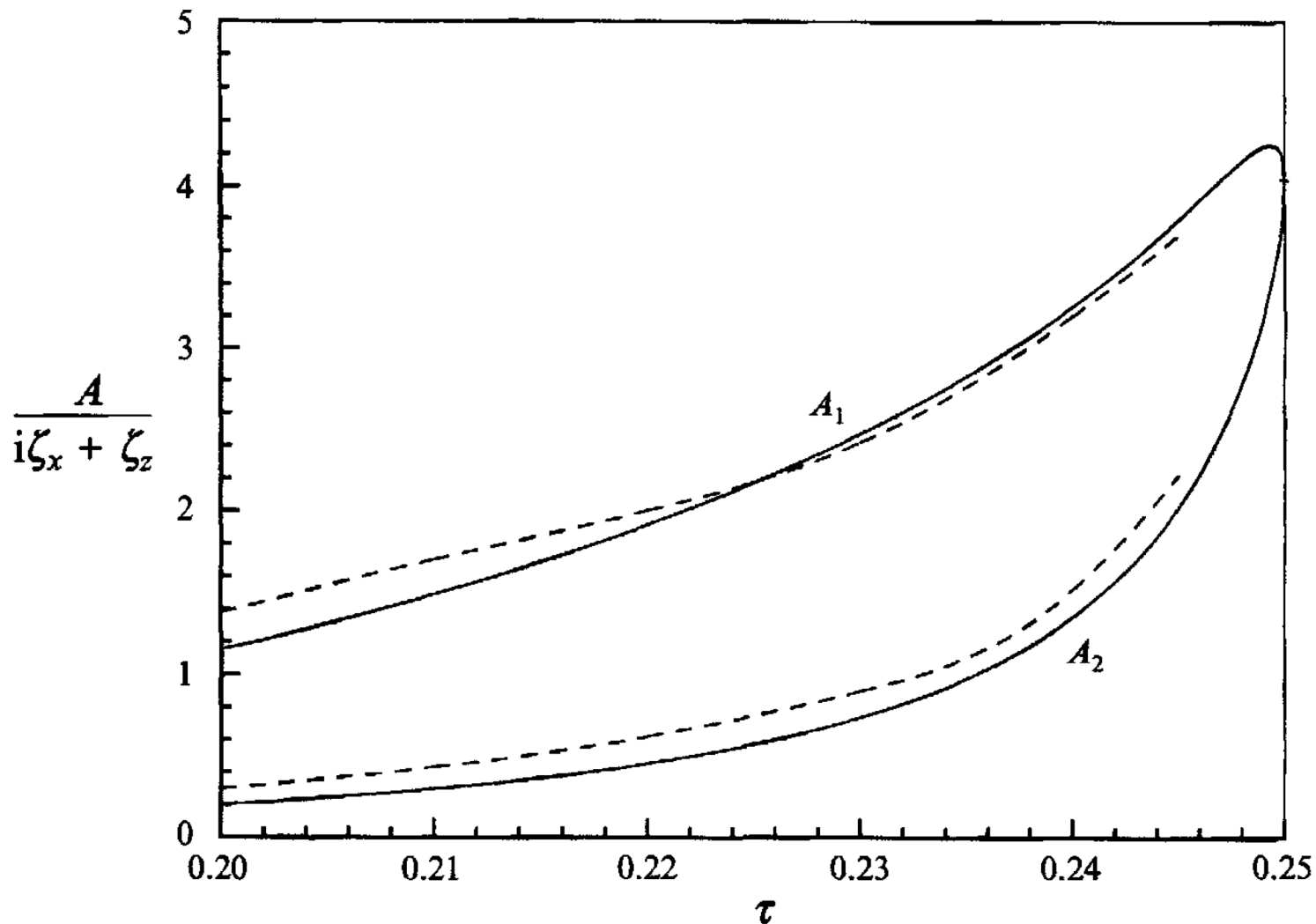
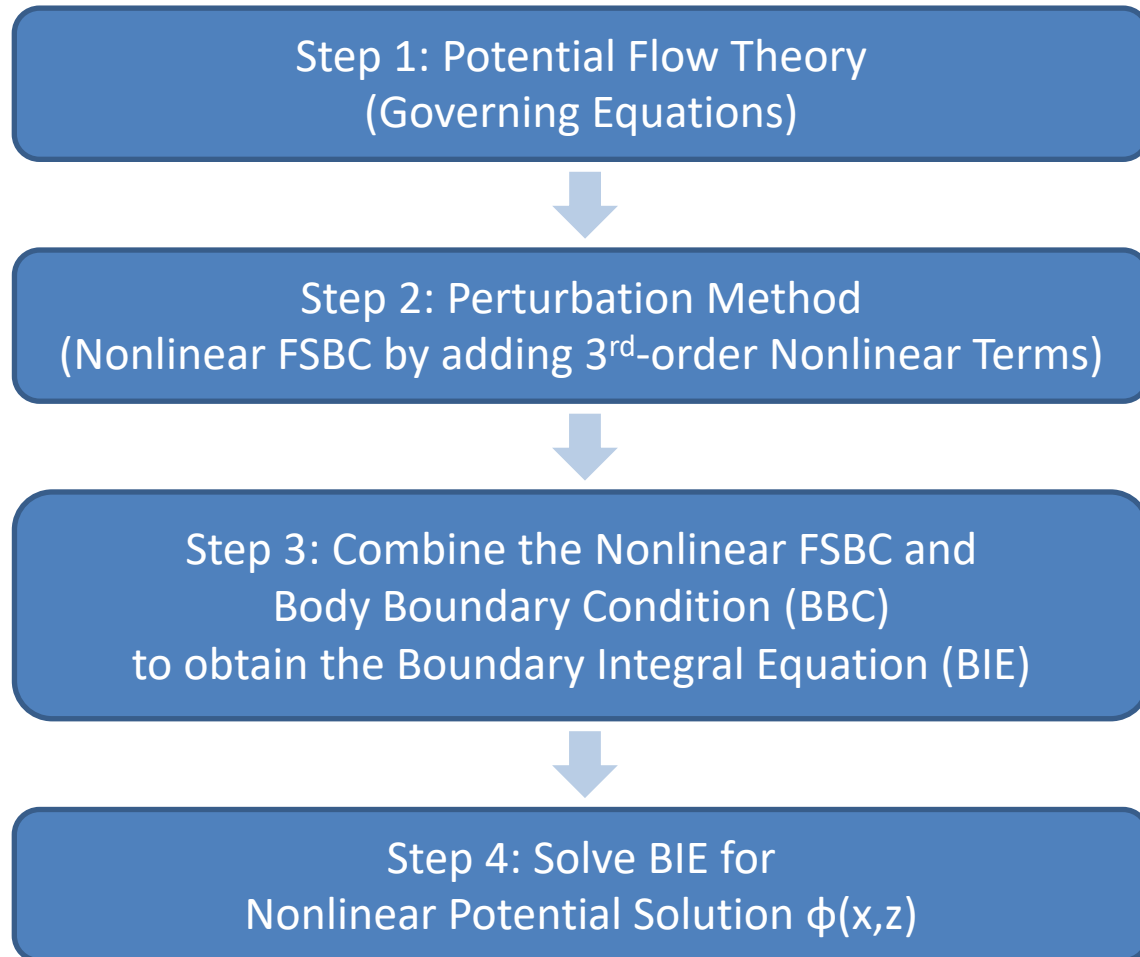


FIGURE 3. Amplitudes of the k_1 (upper branch) and k_2 (lower branch) waves radiated by the heave and sway oscillations of a submerged circular cylinder as a function of $\tau \equiv U\omega/g$. Asymptotic solution (5.13) (—); direct numerical calculations (Grue & Palm 1985) (- - -). ($F_r = U/(gR)^{\frac{1}{2}}=0.4$, $h/R=2$).

Theoretical Analysis of Nonlinear Effects in Frequency Domain



Step 2—Nonlinear Free-Surface Boundary Condition

- Following Dagan & Miloh (1982), for a single source, assumed perturbation for potential: $\phi = \phi_1 + \phi_2 + \phi_3 + \dots$

The analysis showed: $\phi_1 \sim \frac{\epsilon}{\delta}$ $\phi_2 \sim \frac{\epsilon^2}{\delta}$ $\phi_3 \sim \frac{\epsilon^3}{\delta^5}$

When $\delta = \sqrt{1 - 4\tau} \rightarrow 0$: $\frac{\phi_3}{\phi_1} \sim \frac{\epsilon^2}{\delta^4}$ (Non-uniform Convergence)

Perturbation valid only when: $\delta^2 \sim |\epsilon|^\alpha, \alpha < 1$

- Add the **cubic term** to the free surface boundary condition (FSBC) :

$$\underbrace{\frac{\partial^2 \phi_1}{\partial t^2} - 2 \frac{\partial^2 \phi_1}{\partial t \partial x} + \frac{\partial^2 \phi_1}{\partial x^2} + \frac{\partial \phi_1}{\partial z}}_{\text{Linear Terms}} + \underbrace{\frac{1}{2} \nabla \phi_1 \nabla (\nabla \phi_1 \nabla \phi_1)}_{\text{Cubic Term}} = 0 \quad z = 0$$

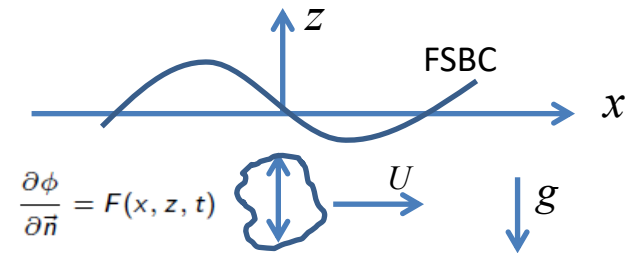
when $\delta = \sqrt{1 - 4\tau} \rightarrow 0$, the magnitude of the cubic term would be comparable with the leading order terms.

$$\frac{\phi_3}{\phi_1} \sim \epsilon^2 \quad (\text{Uniform Convergence})$$

Step 3—Apply Body Boundary Conditions

- Construct the potential solution for a submerged body into two parts:

$$\phi(x, z, t) = \underbrace{\int_{S_B} \sigma(s', t) \ln(r/r_1) ds'}_{\psi(x, z, t) \text{ Source distribution on body surface}} + \underbrace{H(x, z, t)}_{\text{Surface wave effect (free \& evanescent waves)}}$$



Nonlinear FSBC: $H_{tt} - 2H_{tx} + H_{xx} + H_z + \frac{1}{2} \nabla H \nabla (\nabla H \nabla H) = -\psi_z \quad z = 0$

BBC: $\frac{\partial \psi}{\partial n}(x, z, t) + \frac{\partial H}{\partial n}(x, z, t) = F(x, z, t) \quad \text{on } \bar{S}_B$

Here body forcing $F(x, z, t)$ is related to the body velocity and is known.

- Consider steady harmonic oscillation problem: *i.e.* $F(x, z, t) = \Re\{f(x, z)e^{i\omega t}\}$

$$H(x, z, t) = \Re\{h(x, z)e^{i\omega t}\} \quad \psi_z(x, z, t) = \Re\{P(x, z)e^{i\omega t}\} \quad \psi(x, z, t) = \Re\{X(x, z)e^{i\omega t}\}$$

$$\left\{ \begin{array}{l} \text{Laplace Eq.: } h_{xx} + h_{zz} = 0 \\ \text{FSBC: } -\omega^2 h - 2i\omega h_x + h_{xx} + h_z + \frac{1}{2} \nabla h \nabla (\nabla h \nabla h) = -P(x, 0) \quad z = 0 \\ \text{BBC: } X_n(x, z) + h_n(x, z) = f(x, z) \quad (x, z) \in S_B \\ \text{Bottom BC: } \nabla h \rightarrow 0 \quad z \rightarrow -\infty \end{array} \right.$$

Step 4—Nonlinear Solution

- Velocity potential could be obtained:

$$h_{NL}(x, z) = \frac{i2\mathcal{F}(k_c)}{\sqrt{\delta^2 + 4d} + i2k_c\Gamma} e^{-ik_{1g,2g}x + |k_{1g,2g}|z}$$

$$\left\{ \begin{array}{l} \text{Body volume effect: } \Gamma = \int_{S_B} (-in_x + n_z) e^{2k_c z'} ds' \sim O(1); \\ \text{Body forcing: } \mathcal{F}(k_c) = \int_{\bar{S}_B} [f(x, z) - \bar{\mathcal{X}}_n(s)] e^{ik_c x + k_c z} ds. \sim O(\epsilon) \end{array} \right.$$

1. $\Gamma = 0$: $\phi \sim \frac{\tilde{f}}{\sqrt{|\tilde{f}|}} \propto O(\epsilon^{1/2})$ at $\delta = 0$ (i.e. $\tau = 1/4$), consistent with Dagan and Miloh (1982);
2. $\Gamma \neq 0$: total nonlinear solution remain finite, $\phi \propto O(\epsilon)$ at $\delta = 0$ with

$$k_{1g} = \frac{1}{2}(1 - 2\tau + \sqrt{\delta^2 + 4d}); \quad k_{2g} = \frac{1}{2}(1 - 2\tau - \sqrt{\delta^2 + 4d})$$

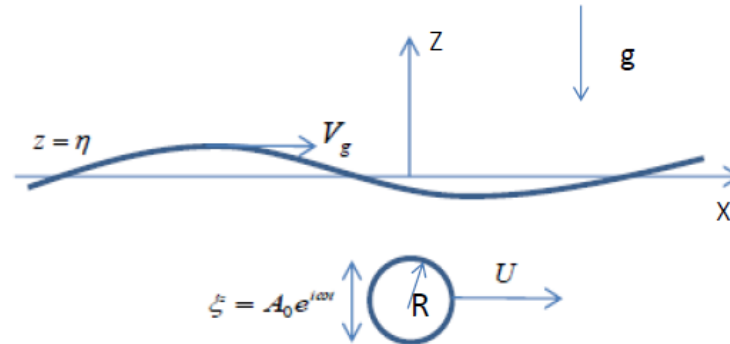
$$d_{1,2} = -\frac{1}{2} \left(\frac{\delta^2}{4} + k_c^2 \Gamma^2 \right) \pm \frac{1}{2} \left[\left(\frac{\delta^2}{4} + k_c^2 \Gamma^2 \right)^2 + 4k_c^4 |\mathcal{F}(k_c)|^2 \right]^{\frac{1}{2}}$$

- Total nonlinear corrections $\propto O(\epsilon)$:

$$h_{COR2}(x, z) = |h_{NL}| - |h_L| \sim \frac{2\mathcal{F}(k_c) e^{k_c z} (e^{\pm \nu x} - 1)}{\delta^2 + 4k_c^2 \Gamma^2} \quad \nu = \text{Im}(\delta^2 + 4d_2)^{1/2} / 2.$$

- ν represents the **nonlinear correction**: spatial damping coefficient to the resonance waves A_1, A_2 .
- **Nonlinear Correction due to cubic interactions is of the same order of magnitude as the leading-order linear solution.**

Analytical Nonlinear Solution for Submerged Circular Cylinder



- Approximation method: treat the potential of steady flow past the circular cylinder as that around a dipole (e.g. Grue & Palm 1984).

$$\begin{cases} \tilde{f} = \pi k_c R^2 e^{-k_c H} (\omega + k_c U) (-\xi_x + i \xi_z) \\ \Gamma = 2\pi R e^{-2k_c H} I_1(2k_c R) \end{cases}$$

- The d term will take the form as:

$$d_2 = -\frac{1}{2} \left[\frac{\delta^2}{4} + 4\pi^2 k_e^2 R^2 e^{-4k_e H} I_1^2(2k_e R) \right] - \frac{1}{2} \left\{ \left[\frac{\delta^2}{4} + 4\pi^2 k_e^2 R^2 e^{-4k_e H} I_1^2(2k_e R) \right]^2 + 16k_e^8 \pi^2 R^4 e^{-2k_e H} (\xi_x^2 + \xi_z^2) \right\}^{\frac{1}{2}}.$$

- The resonant waves $A_{1,2}(x) \sim e^{\nu_{1,2} x}$ with $\nu_{1,2} = \pm \frac{1}{2} \Im(\delta^2 + 4d_2)^{\frac{1}{2}}$

Verification of Analytical Solution for Submerged Circular Cylinder by Comparison with Independent Time-Domain Nonlinear Simulation

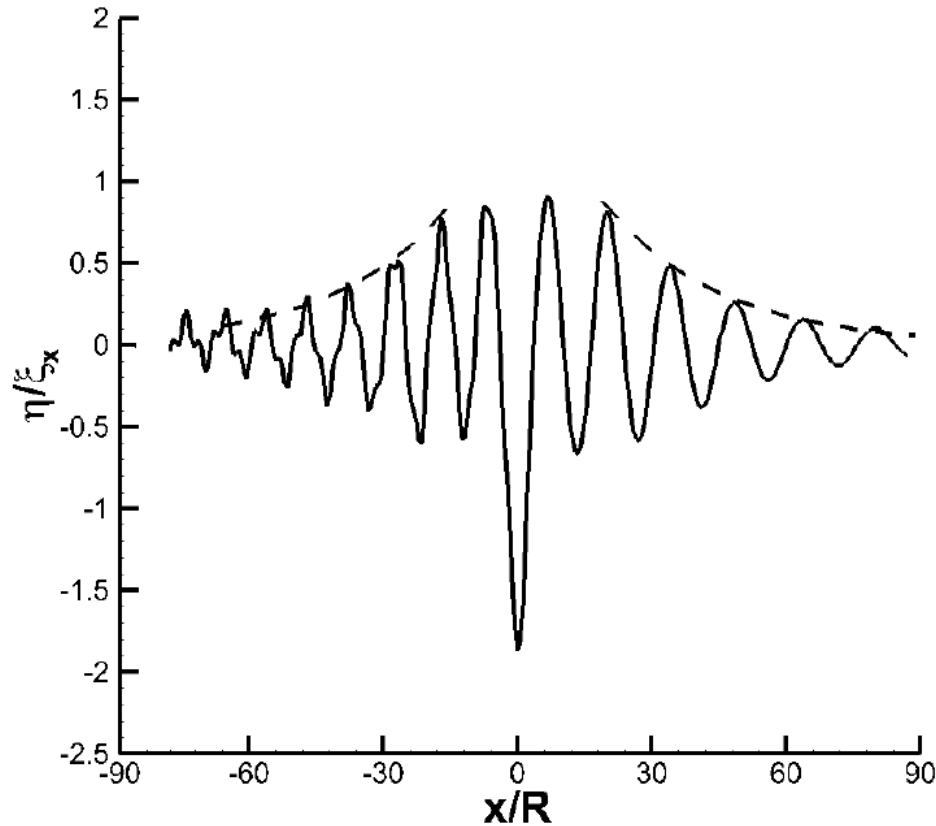


FIGURE 2. Representative instantaneous free-surface shape of steady-state wave profile above the submerged circular cylinder (with its center at $x=0$) obtained by the time-domain nonlinear simulation with $M=3$ (—). Analytical solution of the envelop of decaying wave amplitude of resonant waves at downstream ($x < 0$) and upstream ($x > 0$) of the body $A_{1,2}(x) \sim e^{\pm 0.022x}$ from equation (4.6) (- - -) is also plotted for comparison. ($H/R=6$, $F_r=0.75$, $\tau=0.25$, $\xi_x/R=0.05$).

Verification of Analytical Solution for Submerged Circular Cylinder by Comparison with Independent Time-Domain Nonlinear Simulation

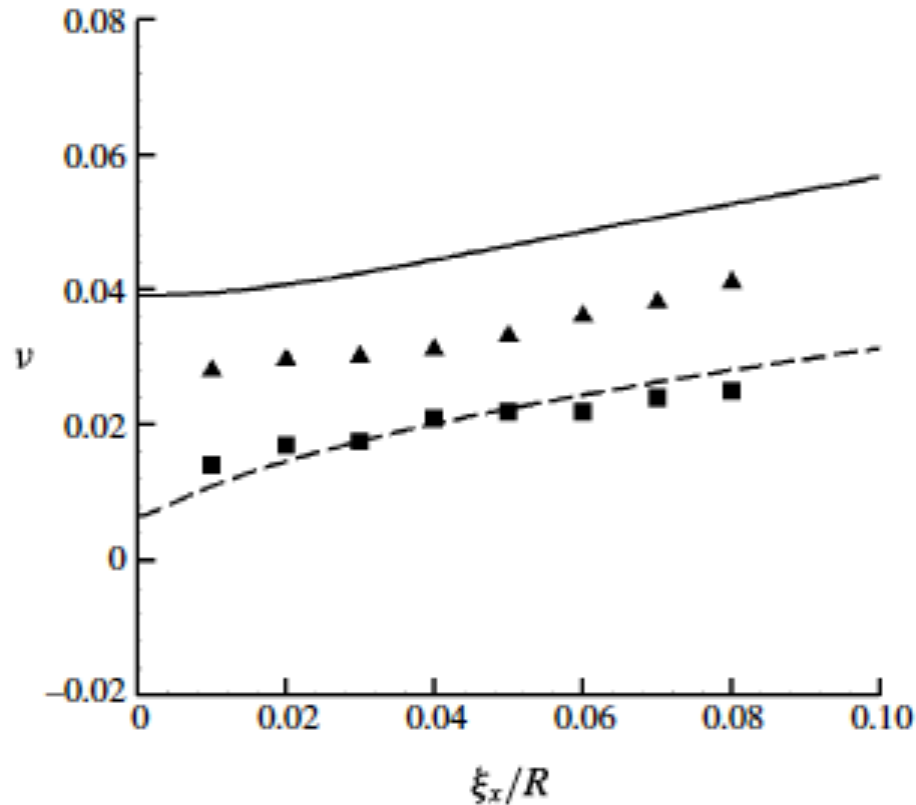


FIGURE 3. Comparison of the damping factor ν_2 of the resonant wave upstream of the body ($A_2(x)$) between the analytic solution from (4.6) with $H/R=4$ (—) and 6 (---), and nonlinear simulations ($M=3$) with $H/R=4$ (\blacktriangle) and 6 (\blacksquare) as a function of the surge motion amplitude ξ_x/R . (Here, $\tau=0.25$ and $F_r=0.75$.)

Verification of Analytical Solution for Submerged Circular Cylinder by Comparison with Independent Time-Domain Nonlinear Simulation

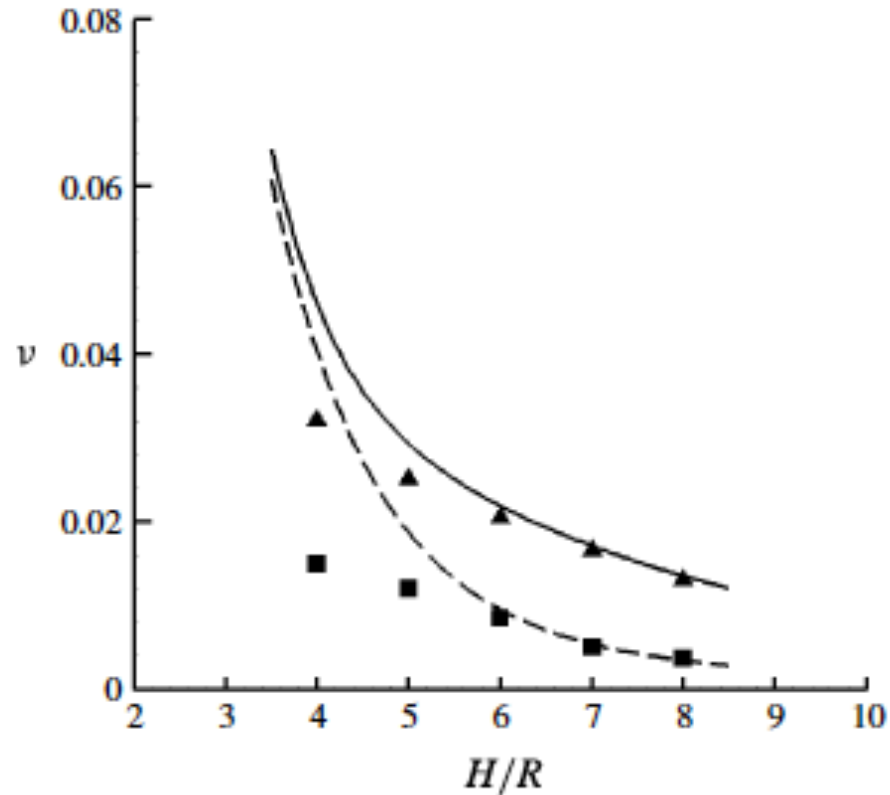


FIGURE 4. Comparison of the damping factor ν_2 of the resonant wave upstream of the body ($A_2(x)$) between the analytic solution from (4.6) at $\tau = 0.245$ (---) and 0.25 (—), and nonlinear simulations ($M = 3$) at $\tau = 0.245$ (■) and 0.25 (▲) as a function of body submergence H/R . (Here, $\xi_x/R = 0.05$ and $F_r = 0.75$.)

Time-Domain Nonlinear Simulation Confirms that Cubic Interactions Gives Leading-Order Contribution at the Critical Frequency

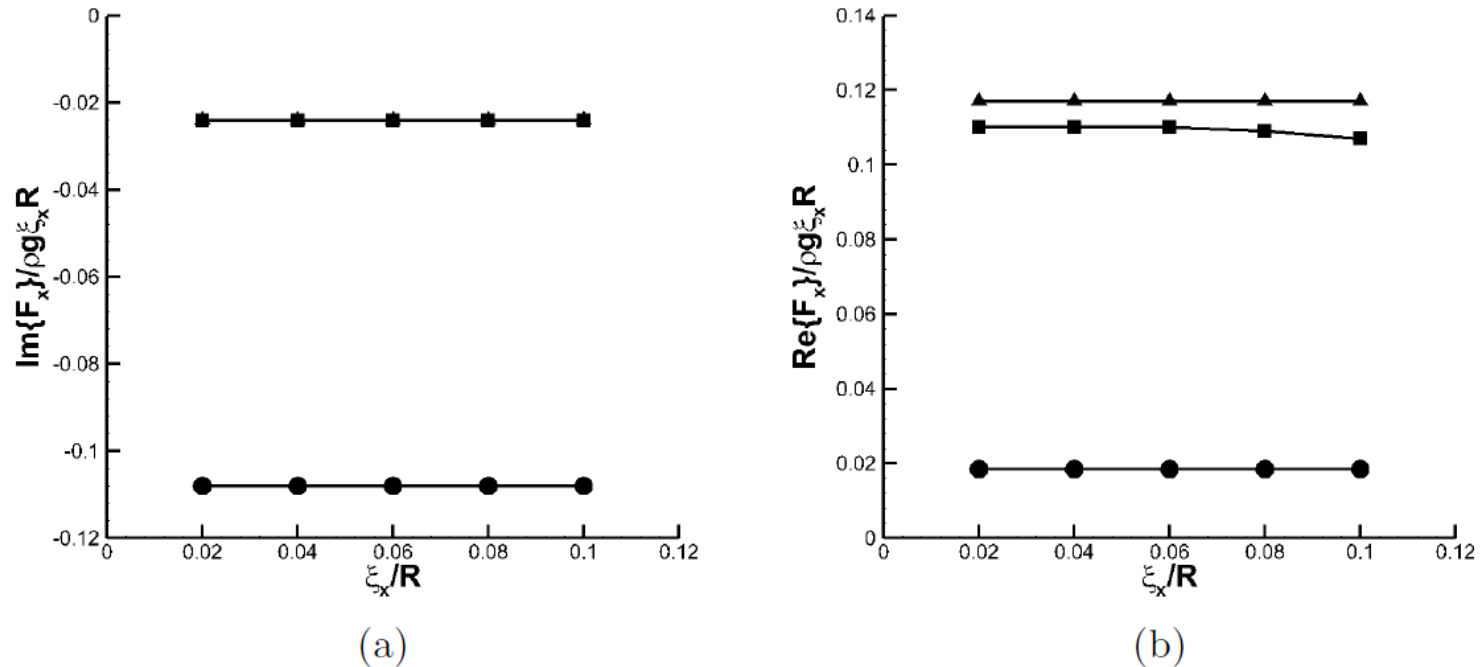


FIGURE 6. The imaginary part (a) and real part (b) of the radiation force in the horizontal direction on the cylinder at $\tau=0.25$ as a function of the surge motion amplitude (ξ_x/R) obtained by nonlinear simulations with $M=1$ (●), 2 (▲), and 3 (■). The results with $M=2$ and 3 overlap each other graphically. ($H/R=6$ and $F_r=0.75$).

Added Mass and Damping Coefficient of S60 Ship at the Critical Frequency by Nonlinear Time-Domain Simulation

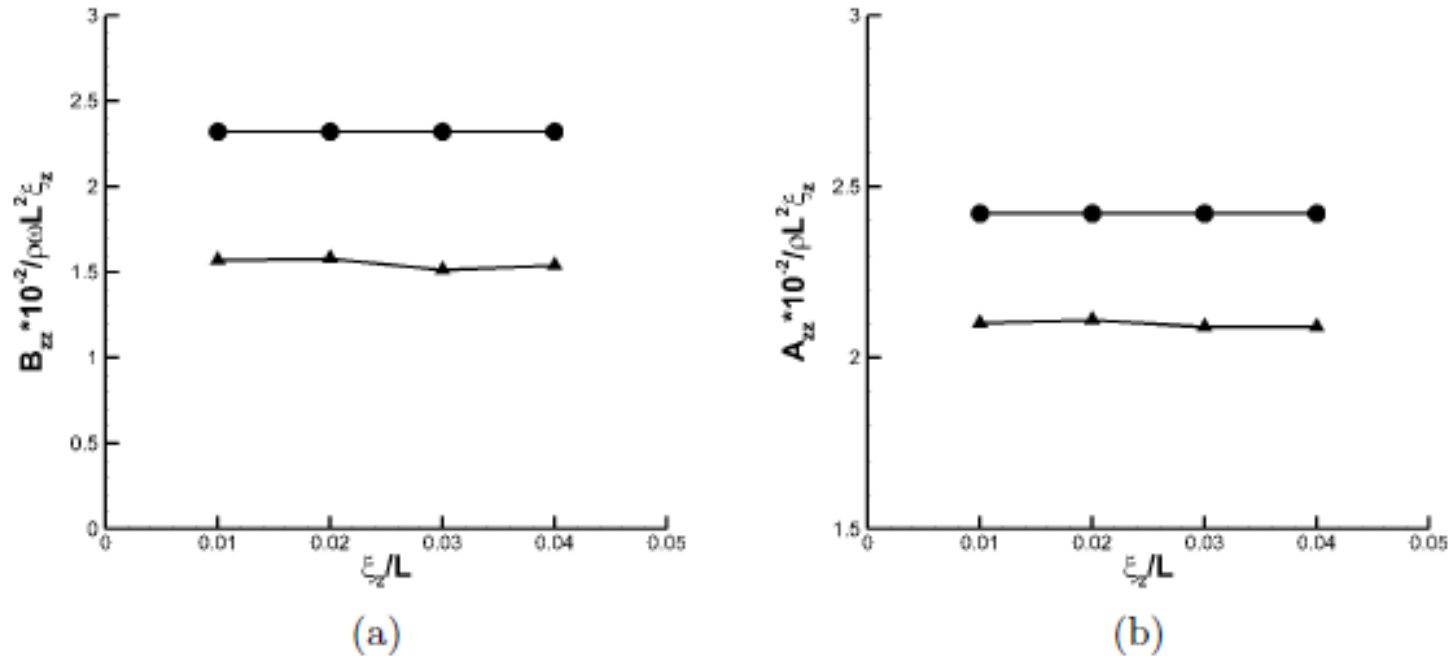


FIGURE 9. Heave damping coefficient (a) and added mass coefficient (b) of a Series 60 ship hull at the critical frequency $\tau=0.25$ as a function of the heave motion amplitude ξ_z/L , obtained by linear (●) and fully-nonlinear (▲) numerical simulations ($F_r=0.2$).

Time Dependence of Wave Resistance of a Body Accelerating from Rest

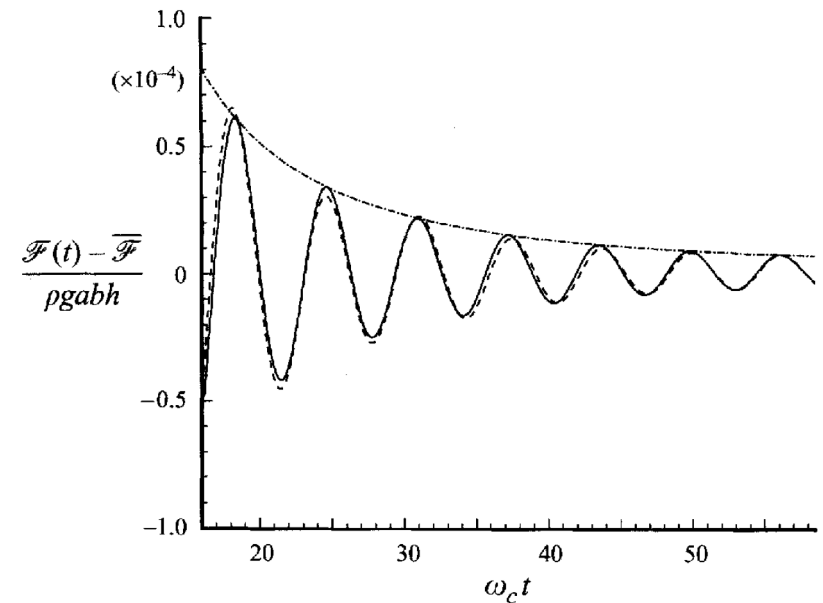
- For a 2D body:

$$\frac{\mathcal{F}(t) - \overline{\mathcal{F}}}{\rho g a^2} = \frac{a_1}{\omega_c t} + \frac{a_2}{(\omega_c t)^{3/2}} \cos(\omega_c t + a_3) \quad \text{for } t \gg 1$$

- For a 3D body:

$$\frac{\mathcal{F}(t) - \overline{\mathcal{F}}}{\rho g a b h} = \frac{a_1}{(\omega_c t)^2} + \frac{a_2}{(\omega_c t)^2} \cos(\omega_c t + a_3)$$

for $t \gg 1$



Comparison between the asymptotic prediction (—) and direct time-domain simulation result (---) for the unsteady wave resistance on a Wigley hull.

Conclusion

For the general 2D and 3D seakeeping problems:

- when $\Gamma \neq 0$, the nonlinear correction due to self cubic interactions of resonant waves near the critical frequency is proportional to $O(\epsilon)$, which is in the same order as the leading-order (linear) solution.
- In the prediction of seakeeping solution near the critical frequency, the nonlinear cubic terms in the free-surface boundary conditions should be included since they will provide the leading-order contribution.

THANK YOU!

QUESTIONS??

Added Mass and Damping Coefficient of S60 Ship near the Critical Frequency by Nonlinear Time-Domain Simulation

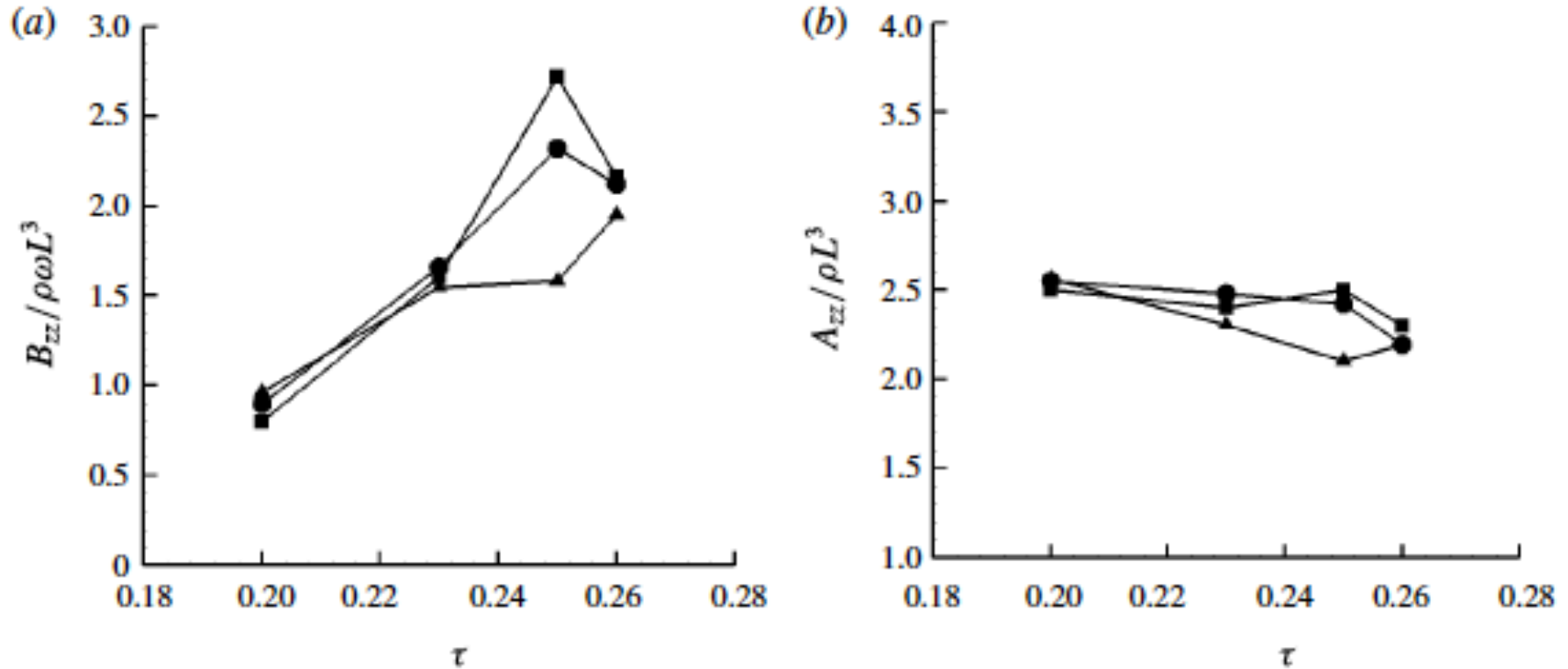


FIGURE 10. The heave damping coefficient (a) and added mass coefficient (b) of a S60 ship hull in the neighbourhood of the critical frequency $\tau = 0.25$ obtained by linear (●) and fully nonlinear (▲) numerical simulations. The linear numerical solution by Bingham (1994) (■) is shown for comparison. (Here, $F_r = 0.2$ and $\xi_z/L = 0.01$.)